

BBA 71487

TUMOR PROMOTER 12-*O*-TETRADECANOYLPHORBOL 13-ACETATE ALTERS STATE, FLUIDITY AND HYDRATION OF 1,2-DIACYL-*sn*-GLYCERO-3-PHOSPHOCHOLINE BILAYERS

PHUONG LAN TRAN ^{a,*}, LISBETH TER-MINASSIAN-SARAGA ^b, GEORGETTE MADELMONT ^b and MONIQUE CASTAGNA ^a

^a Institut de Recherches Scientifiques sur le Cancer, BP8 94802 Villejuif and ^b Laboratoire de Physico-Chimie des Surfaces et des Membranes Equipe de Recherche du CNRS associée à l'Université Paris V, 75270 Paris 06 (France)

(Received June 28th, 1982)

Key words: Diacylphosphatidylcholine; Tumor promoter; Tetradecanoylphorbol acetate; Phase transition; Fluorescence polarization; Differential scanning calorimetry; (Bilayer)

Previous results (Castagna et al. (1979) FEBS Lett. 100, 62–66; Fisher et al. (1979) Biochem. Biophys. Res. Commun. 86, 1063–1068) indicated us that the active tumor promoter TPA (12-*O*-tetradecanoylphorbol 13-acetate) decreased fluorescence polarisation of diphenylhexatriene in lymphoblastoid and rat embryo cells. In the present study, experiments aimed at examining the molecular interactions of tumor promoters with cell membrane components are performed with fully hydrated multibilayers of 1,2-diacyl-*sn*-glycero-3-phosphocholine (DPPC) into which increasing amounts of TPA are inserted. The thermotropic behaviour of both the phospholipid bilayers and the interbilayer water was investigated using the differential scanning calorimetry (DSC) and the approach of Ter-Minassian-Saraga et al. ((1982) J. Colloid Interface Sci. 81, 369–383). The major effects of the tumor promoter are confined to concentrations up to 20% mol fractions of TPA. In this range of concentrations the incorporation of TPA into liposomes decreases the phase-transition temperature but dit not affect ΔH_{DPPC} . Furthermore TPA increases the hydration of the multibilayers. Above 20% mol fractions of TPA, a different thermal behaviour of the system which might suggest morphological rearrangements was observed. The lipid state in TPA-treated liposomes was monitored by fluorescence polarisation using diphenylhexatriene as a lipophilic fluorescent probe and the phase-transition temperature was calculated. The phase transition temperatures determined by both methods were in good agreement. The lowering of this temperature and the decay of fluorescence anisotropy of diphenylhexatriene were parallel. Those effects are consistent with the ‘fluidising’ effect of TPA on DPPC.

Introduction

TPA is the most potent compound within the class of tumor promoters which includes phorbol esters and related macrocyclic diterpenes. Extensive studies on mouse skin [1] and cultured cells

[2,3] strongly suggested that phorbol esters exert their highly pleiotropic cellular effects through the interaction with cell membrane lipid matrix. Phorbol esters are amphipathic compounds which rapidly induce a variety of membrane alterations as reviewed by Weinstein [4] and Blumberg [5]. Some of these effects such as changes in membrane ‘fluidity’, phospholipid turnover and 2-*O*-deoxyglucose uptake occurred in the absence of macromolecular synthesis. Recent reports of study on mouse brain and cultured cells [6–11] have

* To whom all correspondence should be addressed.
Abbreviations: DPPC, 1,2-diacyl-*sn*-glycero-3-phosphocholine; TPA, 12-*O*-tetradecanoylphorbol 13-acetate; 4 α -PDD, 4 α -phorbol didecanoate; DSC, differential scanning calorimetry.

described at least one high affinity phorbol ester-binding site located in cell membranes. The binding to these sites was inhibited by phospholipase A₂ [9]. This strongly suggested that phospholipids were involved in the binding of phorbol esters. Furthermore, it has been shown that phorbol esters incorporated into phospholipid vesicles enhanced the Ca²⁺ efflux mediated by the antibiotic ionophore A 23187 [12]. Good agreement was obtained between this effect and structural requirement of phorbol esters for tumor-promoting activity [13].

Based on the foregoing considerations and using DSC, we studied the effects of TPA on the thermotropic behaviour of fully hydrated multibilayers of DPPC as a model for the lipophilic regions, within the temperature range -60°C to $+60^{\circ}\text{C}$. These studies provided also informations on the thermotropic behaviour of the (structural) water molecules located inside the aqueous gaps separating the bilayers. Parallel studies of fluorescence anisotropy of DPH have also been carried out using the same model system. We report that TPA affects both the state of DPPC acyl chains and the hydration of lipid bilayers.

Materials and Methods

Materials

TPA and DPH were purchased from P. Borchert (Eden Prairie, U.S.A.) and Aldrich Chemical Co. (Beerse, Belgium), respectively. DPPC was purchased from Fluka (Buchs, Switzerland). Its purity was checked by thin-layer chromatography. The solvents, methanol, chloroform and acetone were of spectroscopic grade purity. The phospholipid was dissolved in methanol/chloroform (1:9, v/v) at 8 mg/ml. The concentrations of TPA solutions in acetone were in the range 4–8 mg/ml. The fluorescent probe was dispersed in water to a final concentration of 2 μM according to the procedure of Shinitzky and Barenholz [14].

Preparation of the samples

For DSC studies, samples were prepared as follows: aliquots of DPPC solutions were deposited in Perkin-Elmer aluminium pans and dried under vacuum. Then aliquots of TPA solutions were added and the solvent was evaporated under

vacuum. Both operations were gravimetrically controlled (1 μg accuracy). To the dry lipid (or mixture) weight equal to 0.5 ± 0.005 mg an equivalent amount of water was added. The wet sample was weighed, immediately sealed and reweighed. The samples were incubated at 60°C for 32 h to allow thorough mixing and DPPC and TPA. Sealed samples which lost more than 5 μg after subsequent prolonged heating were discarded. Samples were stored at -18°C . Each experimental condition was scanned in duplicate samples.

For fluorescence emission studies samples were prepared as those used for DSC studies. The dry lipid, pure or mixed with TPA, was allowed to swell in phosphate buffer (pH 7.4) at 50°C . Then vigorous mixing in a vortex mixer yielded multilamellar liposomes. They were used at a final composition of 0.15–0.25 mg/ml. Owing to the very low solubility of TPA in water, $2 \cdot 10^{-6}$ M [15], it is assumed that all TPA was incorporated into the bilayers.

The sample composition was expressed as mol ratio of the lipid and referred to as x_{DPPC} .

Differential scanning calorimetry

DSC thermograms were obtained using a Du Pont de Nemours automatic thermal analyzer and DSC calorimeter type 990-910 equipped with a mechanical cooling accessory. The heating rate was $2 \text{ K} \cdot \text{min}^{-1}$. Sensitivities were 24, 48 and 96 $\mu\text{cal} \cdot \text{s}^{-1} \cdot \text{cm}^{-1}$. The sample and reference cups contained the same amount of water (within $\pm 10 \mu\text{g}$). Heating-cooling cycles were carried out within the temperature range -60°C and $+60^{\circ}\text{C}$. Duplicate scans of each sample were run. The thermograms were analyzed as described in Ref. 16. The onset temperature of the peak on heating mode is taken as the transition temperature t_i . It was obtained by extrapolating to the baseline the ascending branch of the high temperature endothermic peak. This temperature t_i was lower than t_m read at the maximum of the peak. The accuracy was ± 0.25 K. The low transition peaks, endothermic below 0°C and 'exothermic' at 0°C , correspond to the melting of ice inside the sample and inside the reference cups, respectively. The interpretation of these peaks has been given by Ter-Minassian-Saraga and Madelmont [16] and is explained in the Appendix.

Fluorescence measurements

Multilamellar liposomes were loaded with the fluorescent lipid probe diphenylhexatriene. Final molar ratio of probe/lipid was 0.002 (mol/mol). The sample placed in a quartz cuvette was temperature-controlled by circulating water (± 0.1 K). Steady-state fluorescence polarization measurements were performed in a polarization spectrofluorometer (SLM instruments, Champaign, IL), using an excitation wavelength of 366 nm.

The results are expressed in terms of fluorescence anisotropy parameter r as follows:

$$r = (I_{VV} - I_{VHG}) / (I_{VV} + 2I_{VHG})$$

G is a correction factor given by the ratio of the fluorescence intensities of the vertical (V) to horizontal (H) components when the excitation light is polarized horizontally [17]. By measuring the unlabelled samples and buffers, we concluded that background fluorescence and scattering of the excitation light did not interfere with the data (less

than 2%). Depolarization due to the scattering of the emission light was neglected (less than 0.1%).

Excited state lifetime, τ , was measured at 25°C using a flashlamp-excited, Ortec time-resolved fluorometer. The fit between the experimental decay and the reconvoluted curves were analyzed according to Grinvald and Steinberg [18].

Results

DSC thermograms

Fig. 1 shows the thermograms for heating mode obtained with several DPPC + TPA mixed systems at an overall water content of 50% (w/w). Their compositions correspond to the following values of x_{DPPC} : 1, 0.9, 0.8, 0.75 and 0.6. The results corresponding to x_{DPPC} equal to 0.5, 0.25 and 0.15 are not shown. They are very similar to the thermogram obtained for $x_{\text{DPPC}} = 0.6$. Each thermogram displays one high temperature peak and two low temperature peaks (around 0°C). The high temperature endothermic peak corresponds to the DPPC

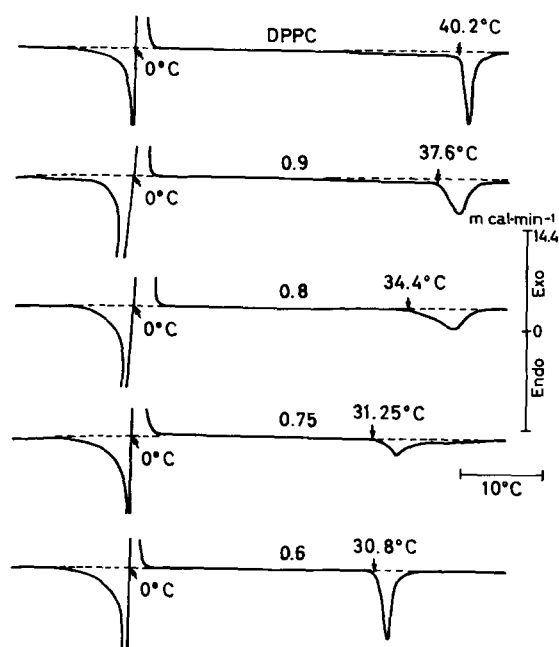


Fig. 1. DSC scans of mixtures of DPPC/TPA. Heating rate, $\text{K} \cdot \text{min}^{-1}$. Sensitivity, $0.2 \text{ mV} \cdot \text{cm}^{-1}$. x , mol fraction of DPPC in dry mixtures. Only temperatures of the onset of the transition t_i are indicated. The weight of DPPC in dry mixtures for mol fractions of 1, 0.9, 0.8, 0.75, 0.6 was: 0.5 mg, 0.457 mg, 0.413 mg, 0.391 mg and 0.321 mg, respectively.

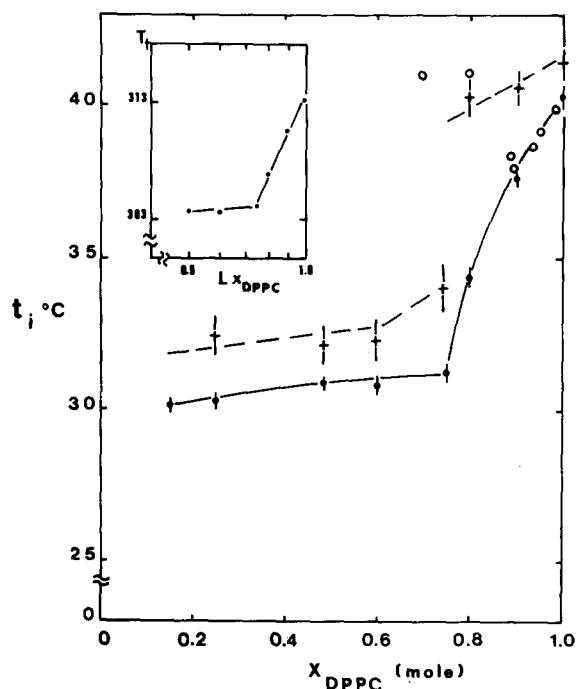


Fig. 2. Phase diagram of hydrated (50%, w/w) DPPC/TPA mixed bilayers transition temperature t_i vs. mol fraction of DPPC as resulting from enthalpic and fluorescence polarization measurements: (●) t_i , (+) t_m , and (○) $t_{1/2}$. Inset: T_i vs. x_{DPPC} .

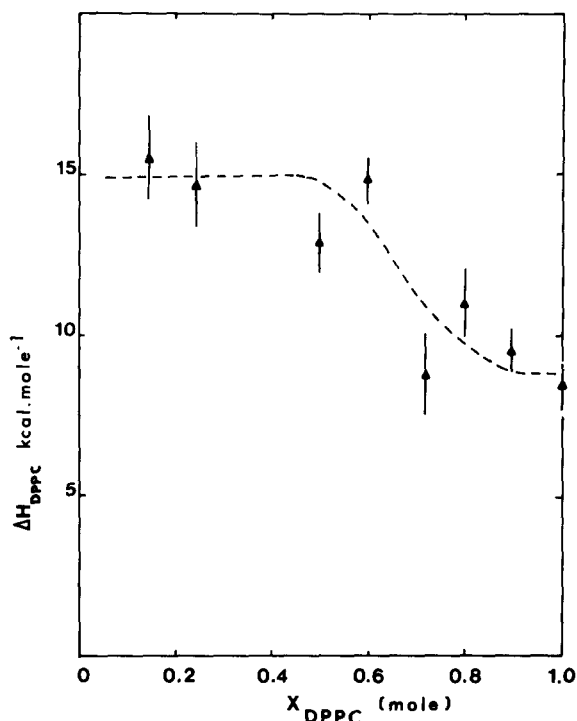


Fig. 3. Variation of the transition enthalpy ΔH (kcal·mol⁻¹) as a function of the composition of DPPC/TPA mixture. x_{DPPC} , mol fraction of DPPC.

gel-liquid crystal transition. The temperatures t_i of the onset of the transition are indicated on each thermogram. Only the thermogram for $x_{\text{DPPC}} = 1$ displays the pretransition peak at 34.0°C (read at the baseline). In the composition range $0.9 \geq x_{\text{DPPC}} \geq 0.8$, the main transition peak broadens and the transition temperature t_i shifts from 40.25°C to 34.4°C. For $x_{\text{DPPC}} = 0.75$ a very broad peak is displayed with a main transition peak at $t_i = 31.25^\circ\text{C}$. For the composition in the range $0.6 \geq x_{\text{DPPC}} \geq 0.15$, this main peak becomes narrower, whereas the corresponding temperature shift is not significant. The difference in the shape of the transition peak for $x_{\text{DPPC}} = 0.75$ and for the other compositions is significant and will be discussed below.

The variation of temperatures t_i and t_m (as defined in Materials and Methods) with bilayer composition is shown in Fig. 2. This figure illustrates the broadening of DPPC main transition peak by TPA. At $x_{\text{DPPC}} = 0.75$, which corresponds to a mol ratio of 1 TPA/3 DPPC, two values of t_m

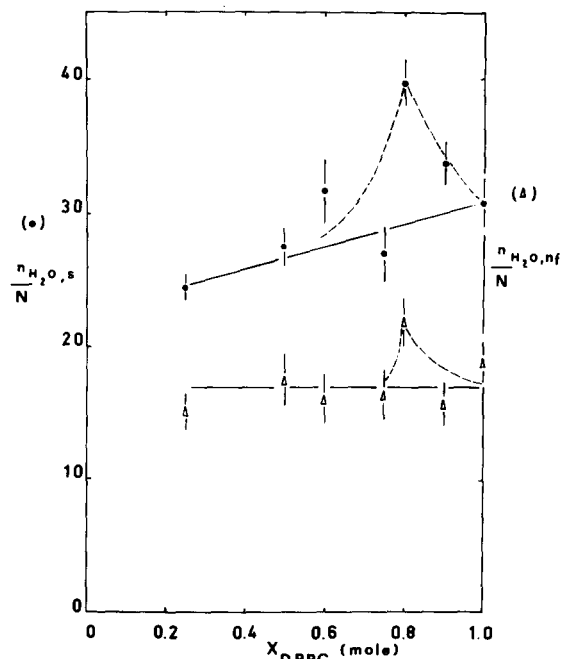


Fig. 4. Effect of composition of DPPC/TPA mixed bilayers on their hydration at 50% (w/w) water content. x_{DPPC} , mol fraction of DPPC; $n_{\text{H}_2\text{O}}/N$, ratio water/lipid (mol/mol). ●, frozen structural water; Δ, non-freezing water.

were observed on the thermogram. In Fig. 2, only the temperature of the first peak is reported ($t_m = 34^\circ\text{C}$). The value for the second peak was not enough resolved.

Molar enthalpies of the DPPC gel-liquid crystal transition derived from the areas of the high temperature endothermic peaks and defined as the enthalpy per mol of DPPC, ΔH_{DPPC} , are shown in Fig. 3. For $x_{\text{DPPC}} = 1$, we obtain 8.4 ± 0.5 kcal·mol⁻¹. This value is consistent with the one previously reported [19]. Following the incorporation of TPA up to a critical composition of $x_{\text{DPPC}} = 0.75$, the effect of TPA on ΔH_{DPPC} is small. On further incorporation of TPA, ΔH_{DPPC} shifted to a higher value 14.5 ± 1.1 kcal·mol⁻¹, independent of x_{DPPC} in the composition range of $0.25 \leq x_{\text{DPPC}} \leq 0.5$.

The low temperature endothermic peak and exothermic peak have been analyzed as reported in the appendix. Two quantities $n_{\text{H}_2\text{O},s}$ and $n_{\text{H}_2\text{O},nf}$ have been obtained. They designate the average number of structural and non-freezing water molecules per molecule in the mixtures, respectively

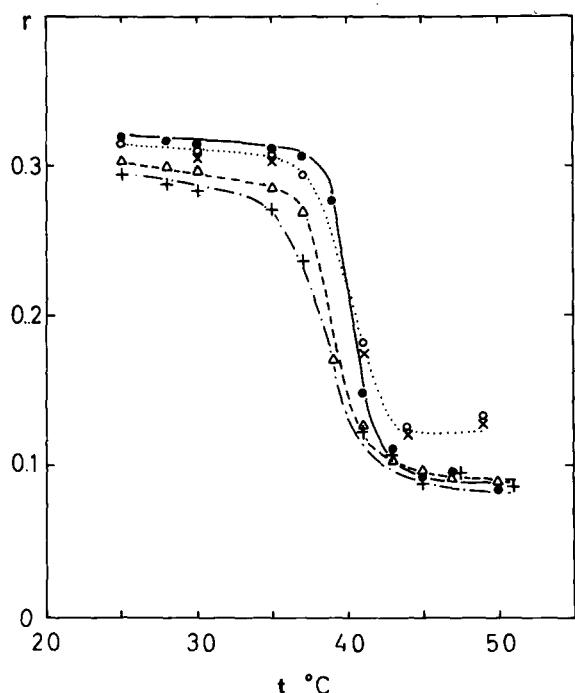


Fig. 5. Temperature profiles of fluorescence anisotropy parameter obtained with diphenylhexatriene-labelled multilamellar liposomes of DPPC containing: no TPA (●), 5% TPA (Δ), 10% TPA (+), 20% TPA (○) and 30% TPA (x).

(Fig. 4). We notice that the shift in $n_{H_2O,s}$ and $n_{H_2O,nf}$ at a TPA incorporation equal to 20% mol fraction is beyond the scatter in the data points. While $n_{H_2O,s}$ decreases on further incorporation of TPA, $n_{H_2O,nf}$ is independent of the amount of TPA.

Fluorescence studies

The fluorescence intensity of the polarized light emitted by labeled mixed liposomes was measured at various temperatures in the range 25–50°C. The plots of fluorescence anisotropy vs. temperature t for liposomes loaded with TPA at mol fractions of 0, 5, 10, 20 and 30%, respectively, are shown in Fig. 5. The transition temperature $t_{1/2}$ obtained from these plots are reported in Fig. 2 along with the results of DSC studies. The results for 1% mol fraction of TPA incorporated into liposomes are not shown.

At 48°C, far above the DPPC transition temperature, TPA does not affect significantly the anisotropy parameter r in the mol fraction range

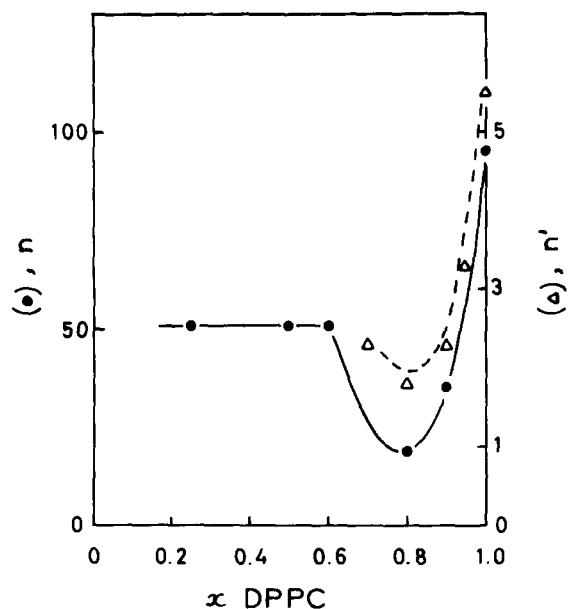


Fig. 6. Variation of n (cooperativity number) vs. x_{DPPC} (●), n calculated from DSC thermograms. (Δ) n' calculated from fluorescence curves.

of $0 \leq x_{TPA} \leq 0.1$. An upward shift of r is observed for $0.2 \leq x_{TPA} \leq 0.3$. In this range the $t_{1/2}$ displays an increase as shown in Fig. 2. For these compositions, the temperature range for the transition is broadened. This result is parallel to the broadening of the transition peaks in the DSC thermograms (Figs. 1 and 2). At 25°C, well below $t_{1/2}$ the shift of the anisotropy parameter r by TPA is within experimental errors in the range of mol fraction $0 \leq x_{DPPC} \leq 0.3$. The excited-state lifetime τ was measured in the absence and the presence of 5% mol fraction of TPA at 25°C. The results obtained, 9.8 ns and 10.6 ns, respectively, indicated that TPA does not modify significantly the lifetime of the probe.

Discussion

The phase diagram t_i and t_m vs. x_{DPPC} (Fig. 2) is plotted using the high temperature peaks of the thermograms shown in Fig. 1. These peaks imply that first order transitions occur in all mixtures studied: $0.15 \leq x_{DPPC} \leq 1$. The inset plot of T_i vs. $\ln x_{DPPC}$, where x_{DPPC} is the mole fraction of DPPC inside the fluid bilayers, verifies the theoretical diagram for gel to liquid crystal transition of

DPPC bilayers in the presence of water-soluble lipophilic molecules expelled from the bilayer gel phase [20]. The analytical form of this diagram is the following:

$$\ln x_{\text{DPPC}} = - \frac{\Delta H_{\text{DPPC}}}{R} \left(\frac{1}{T} - \frac{1}{T_{\text{DPPC}}} \right)$$

where $R = 1.98 \text{ cal} \cdot \text{deg}^{-1}$ is the gas constant and T_{DPPC} the gel-liquid crystal transition of pure DPPC. The slope of the plot, equal to -0.032 , is consistent with the experimental values of $\Delta H_{\text{DPPC}} = 8.4 \text{ cal} \cdot \text{mol}^{-1}$ obtained from the areas of the peaks in the range $0.75 \leq x_{\text{DPPC}} \leq 1$. The molar enthalpy of DPPC transition ΔH_{DPPC} shifts to $14.5 \text{ kcal} \cdot \text{mol}^{-1}$ when x_{TPA} increases from 0.4 to 0.8 mol fraction. Such an effect has been reported for the lipophilic long chain alcohols and tetraalkylammonium salts [21]. In contrast the less lipophilic short chain alcohols lower the value ΔH_{DPPC} . Presumably, these last substances as well as cholesterol [22] might be retained by the DPPC gel phase. The variation of ΔH_{DPPC} with x_{DPPC} rules out the possibility that, for $x_{\text{TPA}} \leq 0.25$ or 1 TPA/3 DPPC, a simple phase separation occurs above the transition temperature t_i . It follows that beyond this concentration of TPA, TPA molecules which have a bulky polar head and only one acyl chain might induce a morphological transition of the bilayers from the lamellar to a more open structure (cylindrical or micellar) of the system. This could be one explanation of the observed shift of ΔH_{DPPC} to $14.5 \text{ kcal} \cdot \text{mol}^{-1}$. Nevertheless further studies are needed to elucidate the behaviour of ΔH_{DPPC} and of the main transition temperature t_i in the range of concentrations $x_{\text{TPA}} > 0.25$.

The change in the morphology of the bilayer might provide an explanation to the results of structural and of non-freezing water studies below 0°C . The structural and non-freezing water gradually decrease between $x_{\text{DPPC}} = 0.8$ and $x_{\text{DPPC}} = 1$. This implies that the aqueous interbilayer separation gradually decreases whereas the acyl chain state changes slowly. Between $x_{\text{DPPC}} = 0.8$ and $x_{\text{DPPC}} = 0.6$ the structural and non-freezing water decrease again. This range of x_{DPPC} values may correspond to some transitory state between two morphological structures. These results obtained for the aqueous spacing between rigid DPPC bi-

layers have been shown to be similar at 0°C and at 25°C [24].

Fluorescence anisotropy obtained with diphenylhexatriene inserted into DPPC bilayers shows that the incorporation of TPA into DPPC liposomes affects mainly the lipid fluid state. The temperature range corresponding to the transition was broadened as for DSC thermograms. The fact that TPA is not incorporated by the gel lipid bilayers at all the concentrations studied is confirmed by the insignificant effect of this molecule on the fluorescence anisotropy parameter r at 25°C . In contrast the upward shift of r at 48°C in the fluid state indicates both the degree of miscibility of TPA within the disordered DPPC paraffin chains and the ordering effect of TPA on these chains.

At high mol fractions of TPA incorporated into DPPC ($x_{\text{TPA}} \geq 0.4$) the thermograms display a sharp transition. We might suggest that TPA may act as a detergent and disperse the DPPC bilayers. Particularly an excess of TPA may form with DPPC mixed micelles or other colloidal structures, whereas at low concentrations ($x_{\text{TPA}} < 0.25$) the incorporation of TPA may produce defects inside the bilayers. These defects may lower the cooperativity of the gel-to-liquid crystal transition of DPPC bilayers. At $x_{\text{TPA}} = 0.25$ the lamellar state may become unstable and the transition to a more open morphology occurs.

We calculated the so-called cooperativity number n according to Hinz and Sturtevant [23], using both our calorimetric and fluorometric data (Fig. 6). For an order-disorder transition (two state process) this number is equal to:

$$n = \frac{4RT_i^2}{\Delta H_{\text{DPPC}}} \left(\frac{d\alpha}{dT} \right)_{T_i} \quad i = m, t$$

where α is the degree of the transition and $(d\alpha/dT)_{T_i}$ is the maximum slope of the plot α vs. temperature T . For pure DPPC our DSC result is consistent with the one previously reported [23]. Smaller values of n obtained from fluorometric measurements could be due to the unaccuracy in the estimation of the slope $(d\alpha/dT)_{T_i}$ inside the transition temperature range. The incorporation of TPA decreases the cooperativity number n significantly. According to Albon and Sturtevant [28],

the number n is defined as a cooperative unit. Thus the observed lowering of n by TPA may correspond to a reduction in the size of the domains or cooperative units. The evolution of the number n with the concentration of TPA may be relevant to the evolution of ΔH_{DPPC} and of the bilayer hydration. We note in particular the singularity for ΔH_{DPPC} and $n_{\text{H}_2\text{O},s}$ at $x_{\text{DPPC}} \approx 0.75$.

Studies of TPA effects on DPPC bilayers at low concentrations of TPA have been carried out by Jacobson et al. [15] and Deleers et al. [25]. These authors have used both techniques DSC and fluorescence polarisation. Their results were not internally consistent [25] and in contrast to their report, Jacobson et al. [15] have shown that TPA and the biologically inactive compound 4α -PDD provided similar thermograms. We could suggest that this similarity reflects the non-specificity of the effects of TPA and inactive analog on DPPC bilayers. As a matter of fact, our DSC measurements and fluorescence polarisation data appear much more consistent to each other. This is probably due to our procedure of sample preparation which is different from the one described in Ref. 25. Our results show that a major change in the state of DPPC occurs at a mol ratio about 1 TPA/3 DPPC, not used by these authors. Furthermore, we would emphasize that in our experimental conditions, we study a TPA concentration range corresponding to 100-fold the active dose for tumor promotion (1–16 nmol). Nevertheless the composition range $0 < \text{TPA/DPPC} \leq 1/10$ (mol/mol) is similar to those required for in vitro cell activity study. Assuming that the membrane lipid amount of a 10^6 cells/ml suspension is in the range 0.002–0.007 $\mu\text{mol/ml}$, the 1/10 TPA/DPPC ratio corresponds to a TPA concentration of about 160 nM. We have shown that under these conditions fluorescence anisotropy parameter changes induced by TPA parallels the TPA binding to fibroblast cell membranes [11]. Unfortunately, since Deleers et al. [25] did not perform binding measurements, we cannot compare our work with theirs.

Whatever the nature of binding site for TPA inside the mosaic fluid biomembrane may be [26], the decay in fluorescence anisotropy of diphenylhexatriene reflects changes in the local packing of

molecules around the probe. These changes are similar to those which are observed following TPA incorporation in our DPPC model membrane.

Appendix

The water content of a sample has been split into interbilayer or internal water and external bulk water. The external water is equal to the amount of water in excess of the amount of the interbilayer or 'structural' water as determined by X-ray (see phase diagrams of Janiak et al. [27]). The frozen structural water melts below 0°C (low temperature endothermic peak); the bulk ice of the sample has a smaller amount of free bulk ice than the reference. This situation is modelled by the 'exothermic' peak at 0°C . This peak is obtained with 0.2 mg of water inside the sample cup and 0.52 mg of water inside the reference cup. The area of this peak corresponds to the mass m_s ($= 0.32$ mg) of pure ice 'missing' in the sample cup. In the case of the hydrated phospholipid samples, which contain the same amount of water as the reference cup the 'missing' ice m_s is constituted by the 'abnormal' interbilayer water which melts below 0°C . Therefore in contrast to Ladbroke et al. [22], our method enables the measurement of the mass m_s of the interbilayer water. The number of interbilayer or structural water molecules $n_{\text{H}_2\text{O},s}$ per lipid molecule is deduced from m_s . If it is assumed [22] that the frozen structural water molecules have a molar enthalpy of melting equal to $L_0 = 1.44 \text{ kcal} \cdot \text{mol}^{-1}$ as for bulk ice, the number of non-freezing water molecules $n_{\text{H}_2\text{O},nf}$ per lipid molecules is deduced from m_s and from the difference between the areas of the 'exothermic' reference peak and of the broad low temperature endothermic peak divided by L_0 .

Acknowledgements

The authors are indebted to Professor J.B. Le Pecq for access to fluorescence equipment and Dr. M. Lebreton for fluorescence excited-state lifetime measurements. This work was supported by D.G.R.S.T. grant 79.7.0795 and I.N.S.E.R.M. grant 118 002.

References

- 1 Van Duuren, B.L. (1969) *Prog. Exp. Tumor Res.* 11, 31–68
- 2 Boutwell, R.K. (1974) *CRC Crit. Rev. Toxicol.* 2, 415–443
- 3 Sivak, A. (1978) in *Carcinogenesis: Mechanism of Tumor Promotion and Cocarcinogenesis* (Slaga, T.J., Sivak, A. and Boutwell, R.K., eds.), Vol. 2, pp. 553–564, Raven Press, New York
- 4 Weinstein, I.B., Mufson, R.A., Lee, L.S., Fisher, P.B., Laskin, J., Horowitz, A.D. and Ivanovic, V. (1980) in *Carcinogenesis: Fundamental Mechanisms and environmental Effects* (Pullman, B., Ts'o, P.O.P. and Gelboin, H., eds.), pp. 543–563, Reidel, Dordrecht
- 5 Blumberg, P.M. (1980) *CRC Crit. Rev. Toxicol.* 8, 153–197
- 6 Driedger, P.E. and Blumberg, P.M. (1980) *Proc. Natl. Acad. Sci. U.S.A.* 77, 567–571
- 7 Estensen, R.D., Dehoogh, D.K. and Cole, C.F. (1980) *Cancer Res.* 40, 1119–1124
- 8 Shoyab, M. and Todaro, G.J. (1980) *Nature* 288, 451–455
- 9 Dunphy, W.G., Delclos, K.B. and Blumberg, P.M. (1980) *Cancer Res.* 40, 3635–3641
- 10 Horowitz, A.D., Greenebaum, E. and Weinstein, I.B. (1981) *Proc. Natl. Acad. Sci. U.S.A.* 78, 2315–2319
- 11 Tran, P.L., Castagna, M., Sala, M., Vassent, G., Horowitz, A.D., Schachter, D. and Weinstein, I.B. (1983) *Eur. J. Biochem.*, in the press
- 12 Deleers, M., Castagna, M. and Malaisse, W.J. (1981) *Cancer Lett.* 14, 109–114
- 13 Hecker, E. (1978) in *Carcinogenesis: Mechanism of Tumor Promotion and Cocarcinogenesis* (Slaga, T.J., Sivak, A. and Boutwell, R.K., eds.), Vol. 2, pp. 11–48, Raven Press, New York
- 14 Shinitzky, M. and Barenholz, Y. (1974) *J. Biol. Chem.* 249, 2652–2657
- 15 Jacobson, K., Wenner, C.E., Kemp, G. and Papahadjopoulos, D. (1975) *Cancer Res.* 35, 2991–2995
- 16 Ter-Minassian-Saraga, L. and Madelmont, G. (1981) *J. Colloid Interface Sci.* 81, 369–383
- 17 Paoletti, J. and Le Pecq, J.B. (1969) *Anal. Biochem.* 31, 33–41
- 18 Grinvald, A. and Steinberg, I.Z. (1974) *Anal. Biochem.* 59, 583–598
- 19 Mabrey, S. and Sturtevant, J. (1976) *Proc. Natl. Acad. Sci. U.S.A.* 73, 3862–3866
- 20 Lee, A.G. (1977) *Biochem. Biophys. Acta* 472, 285–344
- 21 Chen, C.J. (1981) *J. Phys. Chem.* 85, 603–608
- 22 Ladbrooke, B., Williams, R.M. and Chapman, D. (1968) *Biochim. Biophys. Acta* 150, 333–340
- 23 Hinz, H.J. and Sturtevant, J.M. (1972) *J. Biol. Chem.* 247, 6071–6075
- 24 Ter-Minassian-Saraga, L. and Madelmont, G. (1982) *J. Colloid Interface Science* 85, 375–388
- 25 Deleers, M., Defrise-Quertain, F., Ruyschaert, J.M. and Malaisse, W.J. (1981) *Res. Commun. Chem. Pathol. Pharmacol.* 34, 423–439
- 26 Singer, S.J. and Nicolson, G.L. (1972) *Science* 175, 720–731
- 27 Janiak, M.J., Small, D.M. and Shipley, G.G. (1976) *Biochemistry* 15, 4575–4580
- 28 Albon, N. and Sturtevant, J. (1978) *Proc. Natl. Acad. Sci. U.S.A.* 75, 2258–2260